Identifying cancer neighborhoods and cancer-associated fibroblasts in prostate cancer using MERFISH

Jiang He, Ben Patterson, Cheng-Yi Chen
Vizgen®, 61 Moulton St, Cambridge, Massachusetts, United States

vizgen®

Introduction

Understanding the spatial complexities within cancer provides crucial information for evaluating individual tumor development and progression; recent research in prostate cancer has shown how critical it is for oncologists to maintain a spatial context while characterizing a highly heterogeneous tumor microenvironment. As more and more research groups acknowledge the need for spatial biology solutions to solve difficult questions surrounding cell identity, heterogeneity, and interaction, the Vizgen® MERSCOPE® Platform provides a powerful tool to illuminate spatial information. Built on Multiplexed Error-Robust Fluorescence *in situ* Hybridization (MERFISH) technology, MERSCOPE enables the direct profiling of the spatial organization of intact tissue with subcellular resolution. **Here, we use a 500-gene panel to demonstrate the MERSCOPE* Platform's spatial capability, assessing the canonical signaling pathways of cancer, cancer type-specific genes, select immune genes, proto-oncogenes, and tumor-suppressor genes in patient-derived prostate cancer samples.** We found that MERFISH data correlate well with bulk-RNA seq from the same tissue. We were also able to directly profile the *in situ* expression of marker genes for cancer cells, fibroblasts, immune cells, and endothelial cells. Using the MERSCOPE Cell Boundary Stain kit, we were able to generate a molecular and cellular atlas of these individual patient tumors by clustering cells based on gene expression and mapping these clusters back onto a spatial representation of the tumor. **We identified multiple cancer clusters with distinct gene expression profiles and spatial distributions.** Using an alpha shape approach, we marked fibroblasts in the vicinity of cancer neighborhoods (cancer-associated fibroblasts, or CAFs). We identified upregulated genes in CAFs using our MERFISH gene panel as well as Tangram imputation of genome-wide single-cell expression data, which revealed **upregulation of genes related to the extracellular matrix and tumorigenesis.** These findings demonstrate how the MERSCOPE Platform can provide deep insights into the complex heterogeneity observed in the tumor microenvironment.*

**RUO only, not approved for diagnostic or therapeutic purposes*

Materials and Methods

MERFISH is the *in situ* measurement of the expression of hundreds of genes, enabling the visualization of the quantity and distribution of RNA transcripts across a tissue slice. Target RNA species are labeled by tiling oligo probes to barcode each transcript in its native 3-dimensional cellular context. Each barcode is fluorescently detected in sequential rounds of imaging to resolve different RNA species (Figure 1A)[1].

We designed a 500-gene panel targeting canonical signaling pathways of cancer, cancer type-specific genes, select immune genes, proto-oncogenes, and tumor-suppressor genes in a patient-derived FFPE-preserved prostate cancer sample. The sample was prepared using the MERSCOPE FFPE Sample Preparation Kit and the MERSCOPE Cell Boundary Staining Kit to segment cells for further analysis of cell-cell interactions. After MERFISH imaging, decoding, and cell segmentation, data were subjected to further bioinformatic analysis to enable insights into the spatial interactions of different cell populations. For each dataset, 1000-2000 fields of view were captured, generating 10s-100s millions of counts per tissue section. Bulk RNA-seq was performed on the same patient sample for comparison (Figure 1B).

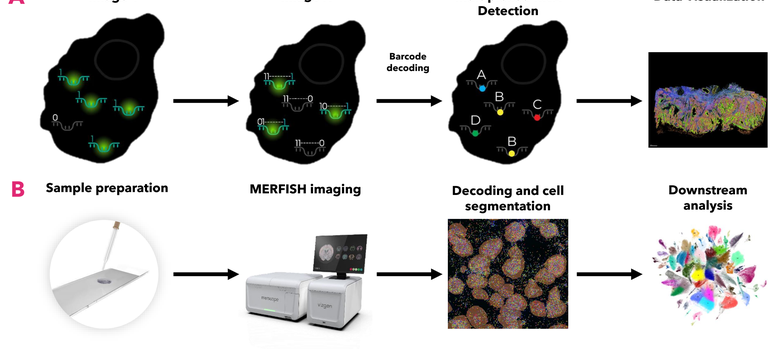

FIGURE 1. MERFISH process and study design. A) During MERFISH, target RNA species are labeled by tiling oligo probes containing different barcodes; each barcode is fluorescently detected in sequential rounds of imaging to resolve the spatial location of different RNA species. **B)** Prepared tissue samples were run on the MERSCOPE® instrument for automated MERFISH imaging, decoding, and cell segmentation before downstream analysis.

Results

MERFISH data correlate with bulk RNA-seq in prostate cancer

MERFISH counts across different gene targets have high concordance with bulk RNA-seq from the same tissue block (Figure 2A). This positive correlation between these orthogonal methods demonstrates the MERSCOPE® Platform's capability for highly accurate data capture in patient-derived tumor samples. The platform's high detection efficiency is illustrated by the reliable detection of lowly expressed genes. MERFISH concordance with bulk RNA-seq exceeds the concordance between RNA-seq technical replicates (Figure 2B).

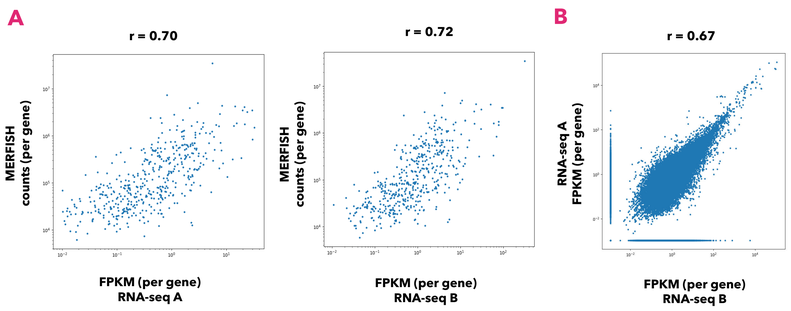

FIGURE 2. MERFISH data correlate with bulk RNA-seq in patient-derived prostate cancer tissue. A) MERFISH data show high concordance (Pearson's correlation coefficient) with two RNA-seq experiments from the same tissue block. **B)** The concordance between both RNA-seq experimental replicates is also illustrated. Reference data comparing MERFISH to RNA-seq and sc-RNA-seq in mouse brain and liver have been published[2].

MERFISH imaging of genes linked to prostate cancer progression and carcinogenesis

The MERSCOPE® Vizualizer was used to spatially assess the transcript distribution of prostate cancer-associated genes *CD276*, *CDH1*, and *PLA2G2A*[3,4]. The spatial distribution of these genes across the tumor region reflected the classical prostate cancer morphology observed in this sample (Figure 3A). Fibroblast-related expression is visualized in the same region by *COL1A1* and *COL4A1*[5], as are vascular endothelium using *PECAM* and *VWF* (Figure 3B)[6]. CXCR3 ligands including *CXCL9*, *CXCL10* and *CXCL11* form "immunity hubs" and a representative immune hub (co-positive for *HLA-DRA* and *C1QC*) is depicted (Figure 3C)[7-9].

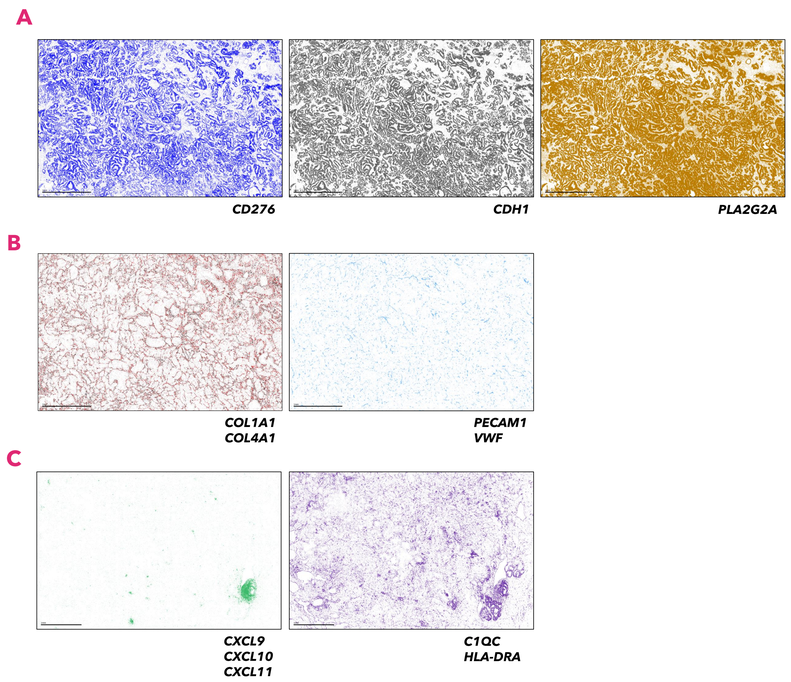

FIGURE 3. *In situ* profiling for marker genes in prostate cancer using MERFISH. A) Spatial distribution of prostate cancer-associated genes *CD276*, *CDH1*, and *PLA2G2A*. **B)** Fibroblast-related gene expression is visualized in the same region as (A) using the genes *COL1A1* and *COL4A1*. Vascular endothelium are visualized in the same region as (A) using the genes *PECAM1* and *VWF*. **C)** An immune hub marked by *CXCL9*, *CXCL10*, *CXCL11* is shown from a different region; the hub is additionally marked by *C1QC* and *HLA-DRA* expression.

Identifying molecularly distinct cell types in prostate cancer

We were able to segment cells[10] across the tissue slice based on the cell boundary stain using the MERSCOPE® Cell Boundary Staining Kit and DAPI staining (Figure 4A). Unbiased clustering of segmented cells revealed 28 cell clusters that were re-mapped to their original spatial locations in the tissue context (Figure 4B). Specific cell types could then be further annotated based on the gene expression profile (Figure 4C). The dendrogram correctly segregates cancer clusters from somatic tissue. The specific cell types were then re-mapped onto the UMAP and spatial tissue representations (Figure 4D). The major regions of cancer cell localization can be readily identified from the spatial representation. A representative zoomed-in image with the 3 cancer meta-clusters illustrates the heterogeneity present in the tumor landscape that was captured by MERFISH (Figure 4E).

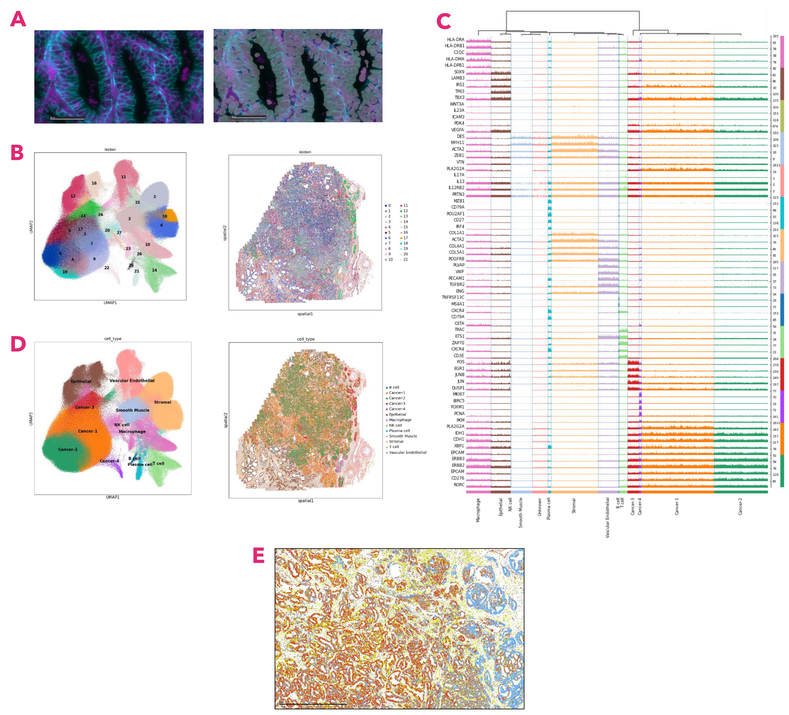

FIGURE 4. MERFISH identifies molecularly distinct cell types in prostate cancer tissue. A) Field of view illustrating cell boundary (teal) and DAPI (fuchsia) staining, facilitating cell segmentation (segmented cells highlighted in grey). Scale bar is 50 µm. **B)** Unbiased clustering of cells identified 28 clusters (left) that were re-mapped spatially back into the tissue context (right). **C)** Track plot showing the clustering and identification of specific cell types from the unbiased clusters. Tracks show gene expression from all cells in each cell type for a given 5 top genes per cell type. **D)** Re-mapping of cell type clusters onto the Leiden UMAP space (left) and spatial tissue representation (right). **E)** Example image of the meta-clusters Cancer-1 (red), Cancer-2 (yellow), and Cancer-3 (blue). Scale bar represents 1 mm.

Identifying cancer neighborhoods and cancer-associated fibroblasts; upregulation of reactive stroma genes in CAFs

Using an alpha shape approach, we identified cancer neighborhoods and fibroblast cells in the vicinity of cancer cells (cancer-associated fibroblasts, or CAFs). To investigate the up-regulated genes in CAFs we performed differential expression (DE) analysis comparing fibroblasts inside vs outside the cancer neighborhood. An additional round of DE was performed to ensure that up-regulated genes in CAFs are also up-regulated compared to cells that neighbored CAFs. We identified the upregulation of several reactive stroma genes in CAFs. The upregulation of reactive stroma genes such as *PDGFRB*, *ENG*, *TGFB1*, *TGFB2*, and *WNT5A* indicate the production of reactive signals by CAFs, a process known to occur during epithelial cell transformation[11].

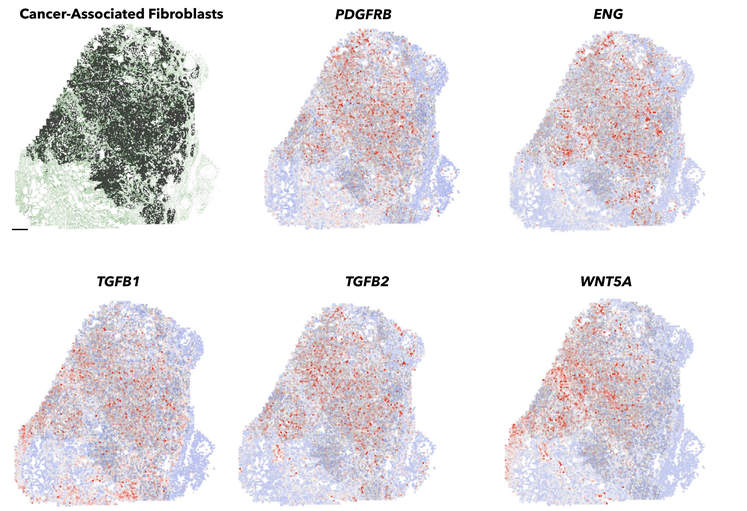

FIGURE 5. MERFISH identifies upregulated genes in CAFs. Representative examples of genes upregulated in fibroblasts versus cells outside the neighborhood are depicted using a hex-tile approach (Z-score of mean fibroblast gene expression in each tile); red/blue for positive/negative, respectively. Top left image: fibroblasts (green dots) located inside and outside the cancer neighborhood (dark grey region). Remaining images: Grey depicts the cancer neighborhood, and red hexagons denote fibroblasts. Scale bar is 1 mm.

Identification of up-regulated imputed genes in CAFs

Using Tangram[12] to impute genome wide single-cell expression, we were able to generate transcriptome-wide spatial data. This helped us to identify up-regulated genes in CAFs not measured by MERFISH. These included several extracellular matrix (ECM) related genes (*MMP19*, *FBLN5*, *COL15A1*) that could be evidence of tumor-related tissue remodeling and genes with prior associations with CAFs or fibroblast function (*CXCL14*, *ITGA11*)[13, 14]. The spatial relationships between CAFs and the ECM remodeling they direct within the tumor-enriched regions of the patient sample could provide crucial information to researchers about CAF-tumor cell crosstalk.

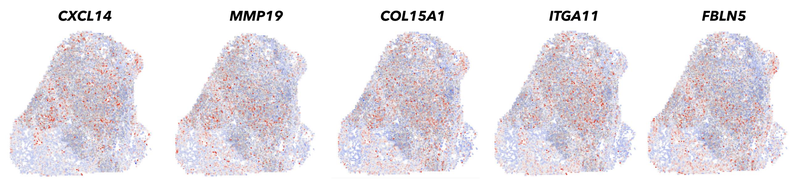

FIGURE 6. Using imputation to identify up-regulated genes in CAFs . Tangram imputation of genome wide single-cell expression data identified several upregulated genes. Representative examples of genes upregulated in CAFs are depicted using a hex-tile approach (Z-score of mean fibroblast expression in each tile); red/blue for positive/negative. Scale bar is 1 mm.

Conclusions

1. We used MERFISH to profile the expression of 500 genes related to canonical signaling pathways of cancer, immune function, and oncogenes in a patient-derived prostate cancer tumor.
2. Gene expression detected on the MERSCOPE® Platform recapitulates data from bulk RNA-seq.
3. We spatially mapped gene expression and cell populations onto a 3-dimensional image of the prostate cancer tissue sample.
4. We identified several molecularly distinct cell types in prostate cancer, with sufficient data to detect multiple cancer subpopulations within the tumor. This detailed cell atlas revealed insights into cell-cell interactions and tumor progression dynamics.
5. We identified populations of CAFs that displayed an upregulation of reactive stroma genes.
6. Using imputation, we generated transcriptome-wide spatial data and identified up-regulated genes in cancer-associated fibroblasts.

References

1. Spatially resolved, highly multiplexed RNA profiling in single cells (2015). DOI: 10.1126/science.aaa6090.
2. Concordance of MERFISH spatial transcriptomics with bulk and single-cell RNA sequencing. DOI: 10.26508/lsa.202201701.
3. Tumor B7-H3 expression in diagnostic biopsy specimens and survival in patients with metastatic prostate cancer. https://doi.org/10.1038/s41391-021-00331-6
4. The Immunotherapy and Immunosuppressive Signaling in Therapy-Resistant Prostate Cancer. https://doi.org/10.3390/biomedicines10081778
5. Fibroblasts: Origins, definitions, and functions in health and disease. https://doi.org/10.1016/j.cell.2021.06.024
6. Vascular Endothelial Cells: Heterogeneity and Targeting Approaches. https://doi.org/10.3390/cells10102712 .
7. Interferon-γ-Inducible Chemokines as Prognostic Markers for Lung Cancer. https://doi.org/10.3390/ijerph18179345
8. Spatially organized multicellular immune hubs in human colorectal cancer. https://doi.org/10.1016/j.cell.2021.08.003.
9. PD-L1 Dependent Immunogenic Landscape in Hot Lung Adenocarcinomas Identified by Transcriptome Analysis. https://doi.org/10.3390/cancers13184562.
10. Cellpose: a generalist algorithm for cellular segmentation. https://doi.org/10.1038/s41592-020-01018-x.
11. Stromal fibroblasts in cancer initiation and progression. doi: 10.1038/nature03096.
12. Deep learning and alignment of spatially resolved single-cell transcriptomes with Tangram. https://doi.org/10.1038/s41592-021-01264-7
13. CXCL14 is an autocrine growth factor for fibroblasts and acts as a multi-modal stimulator of prostate tumor growth. doi: 10.1073/pnas.0813144106.
14. Integrin alpha 11 in the regulation of the myofibroblast phenotype: implications for fibrotic diseases. https://doi.org/10.1038/emm.2017.213.

Learn More